Supplementary Material

Aromatic/Aliphatic residue balance regulates Cu(II)-induced supramolecular gel formation and drug release in histidine-containing tetrapeptides

Kenta Fukumoto, Asuka Inada*, and Tatsuya Oshima

Department of Applied Chemistry, Faculty of Engineering, University of Miyazaki, 1-1 Gakuen Kibanadai Nishi, Miyazaki 889-2192, Japan

*Corresponding author: a.inada@miyazaki-u.ac.jp

Table of Contents

Experimental procedures

Peptide synthesis

The peptides l-His-l-Ile-l-Ile-l-Ile (HIII), l-His-l-Ile-l-Ile -l-Phe (HIIF), l-His-l-Ile -l-Phe-l-Phe (HIFF), and l-His-l-Phe-l-Phe -l-Phe (HFFF) were synthesized using a standard Fmoc solid-phase peptide synthesis (SPPS) strategy. Peptide elongation was performed from the C-terminus to the N-terminus using Fmoc-protected amino acids on Fmoc–amino acid–Wang resin. Prior to synthesis, the resin was swollen in dichloromethane (DCM) for 1 h. Coupling reactions were performed using three equivalents of Fmoc-protected amino acids (relative to the resin-bound amino group), three equivalents of COMU dissolved in N,N-dimethylformamide (DMF), and four equivalents of 2,4,6-trimethylpyridine (TMP) in N-methyl-2-pyrrolidone (NMP). The coupling step was repeated until a negative Kaiser test was obtained. Fmoc deprotection was achieved by treatment with a 20% (v/v) piperidine solution in DMF for 10 min. After completion of the synthesis, the resin was washed three times with DMF, followed by three washes with DCM and one wash with methanol, and then dried under reduced pressure. Cleavage of the peptide from the resin and simultaneous side-chain deprotection were performed using a precooled (4 °C) cleavage cocktail consisting of trifluoroacetic acid (TFA), triisopropylsilane (TIPS), and H2O in a volume ratio of 95:2.5:2.5 for 90 min at room temperature. The resulting peptide solution was precipitated by addition of 20 volumes of diethyl ether precooled to 0 °C and collected by centrifugation at 5000 × g for 10 min. The dissolution–precipitation procedure was repeated three times, after which the residue was air-dried for at least 2 h. The crude peptide was then redissolved in a small amount of water and lyophilized. Finally, the TFA counteranions of the resulting peptide were removed using an anion-exchange resin. Peptide purity was analyzed by reverse-phase high-performance liquid chromatography (RP-HPLC) using a Shimadzu Prominence gradient system (Kyoto, Japan) equipped with a C18 column (Asahipak ODP, 5 µm, 4.6 mm × 250 mm). Isocratic elution was performed with acetonitrile and water as mobile phases A and B, respectively, both containing 0.1% (v/v) TFA. The flow rate was set to 1.0 mL/min (A:B = 8:2), and the column temperature was maintained at 40 °C. Detection was performed at 220 nm using a Shimadzu SPD-20A UV–vis detector. The purities of the resulting peptides (HIII, HIIF, HIFF, and HFFF) were determined to be 95.9%, 92.3%, 92.1%, and 97.0%, respectively (Fig. S1). Their identities were confirmed by Q-Exactive mass spectrometry (Thermo Fisher Scientific Inc., Waltham, MA, USA).

Supporting Figures

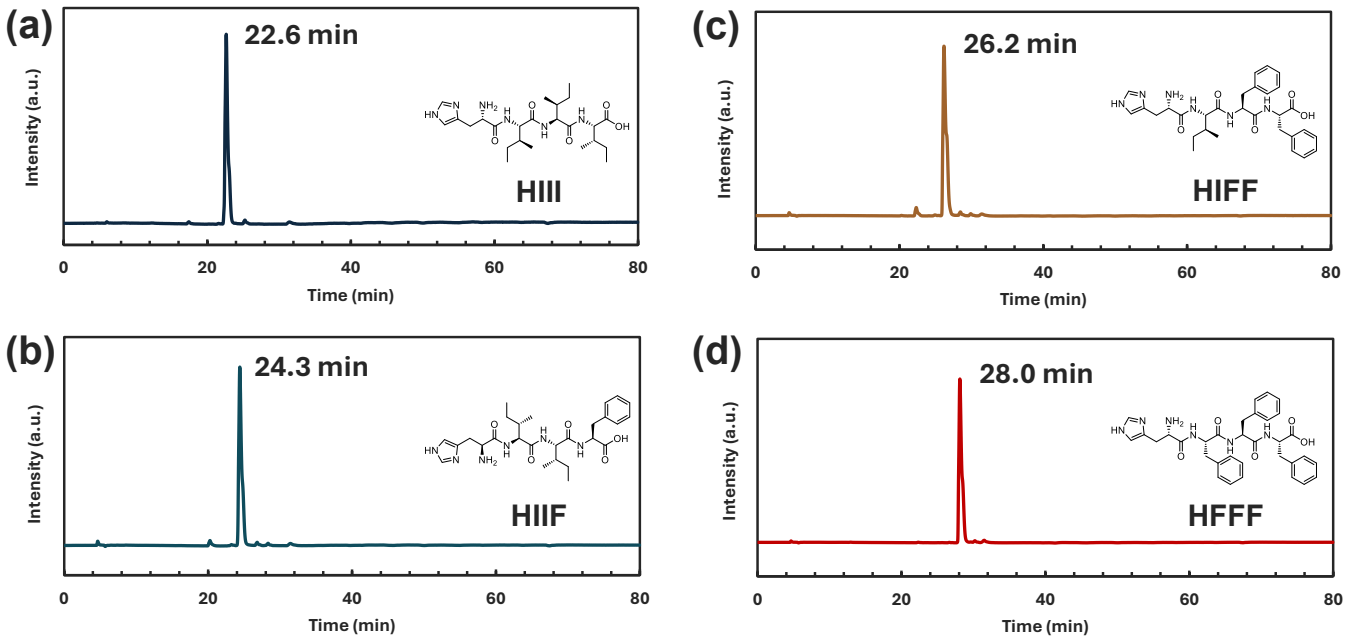

Fig. S1 Baseline-corrected HPLC pattern of the synthesized peptides (a) HIII, (b) HIIF, (c) HIFF, and (d) HFFF; the retention time increased with increasing number of Phe residues in the peptide sequence.

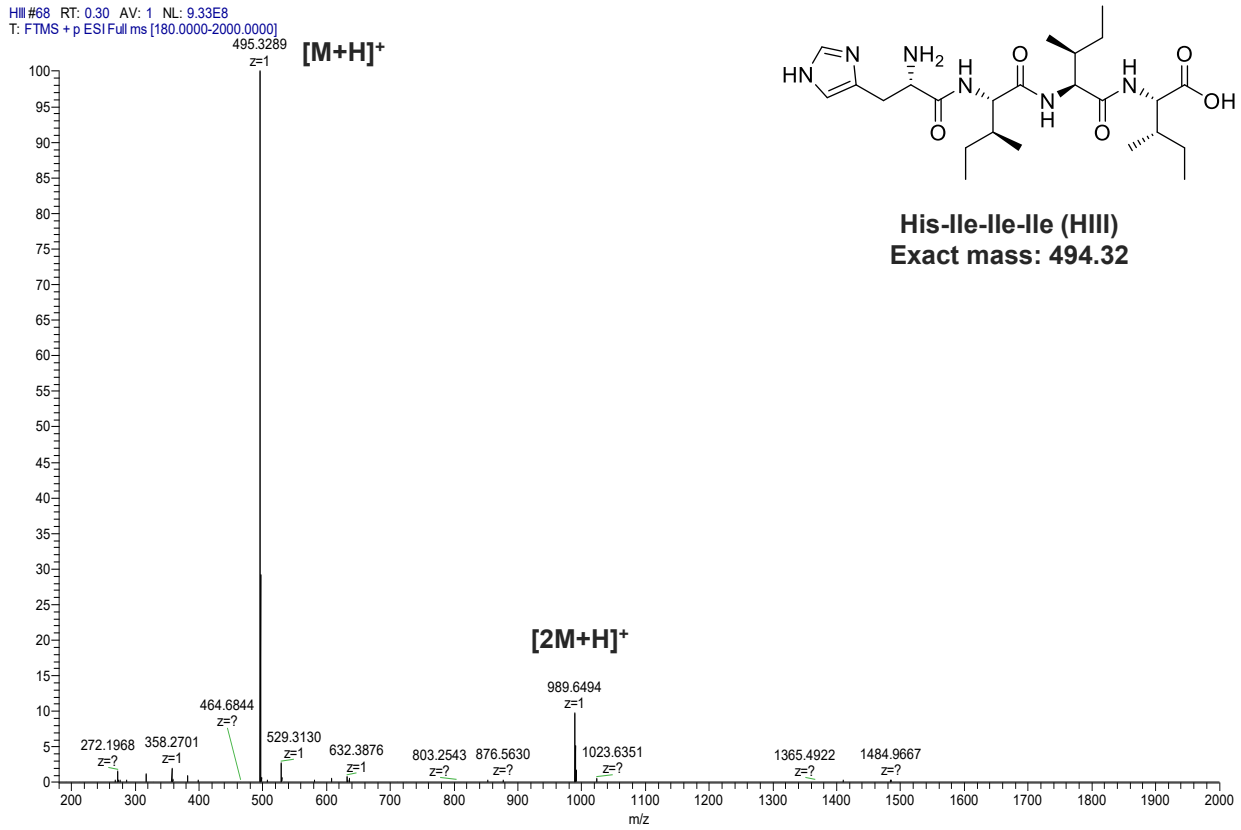

Fig. S2 ESI-TOF MS spectrum of the synthesized peptide HIII

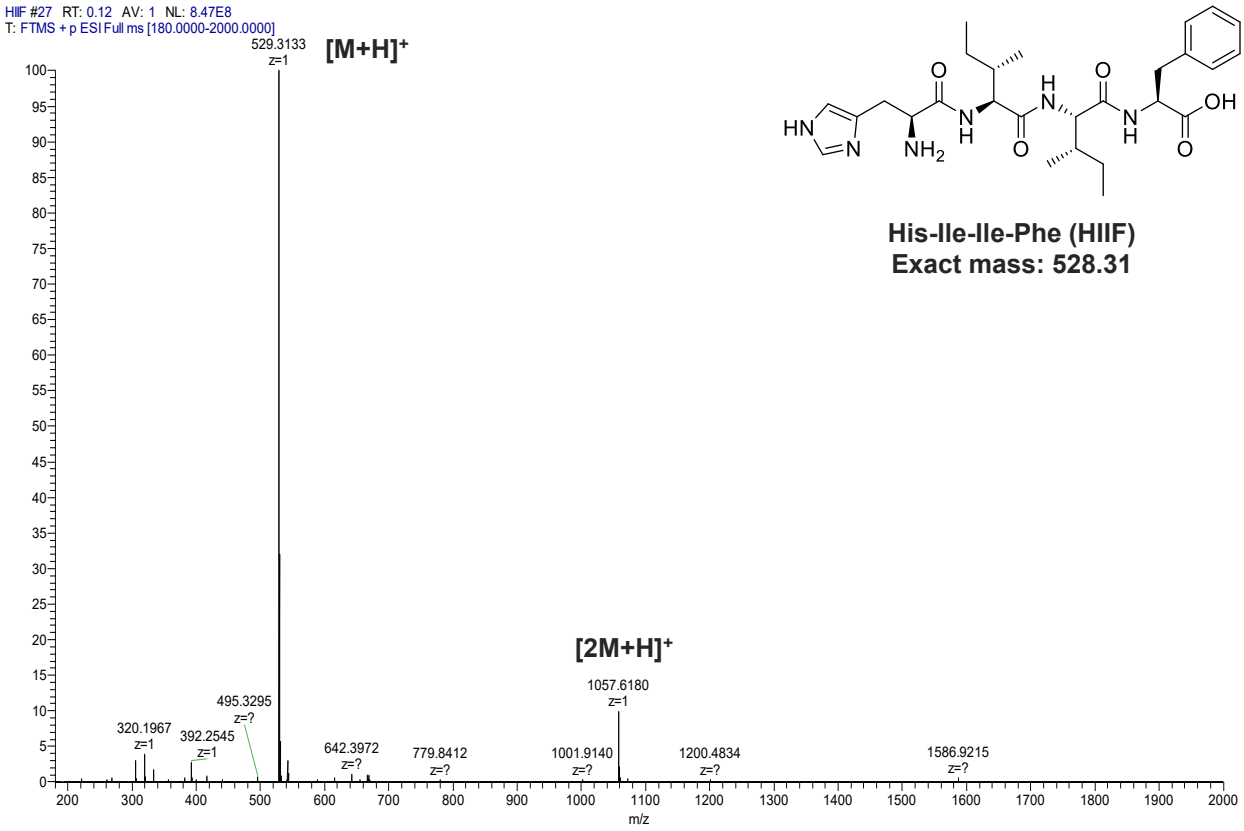

Fig. S3 ESI-TOF MS spectrum of the synthesized peptide HIIF

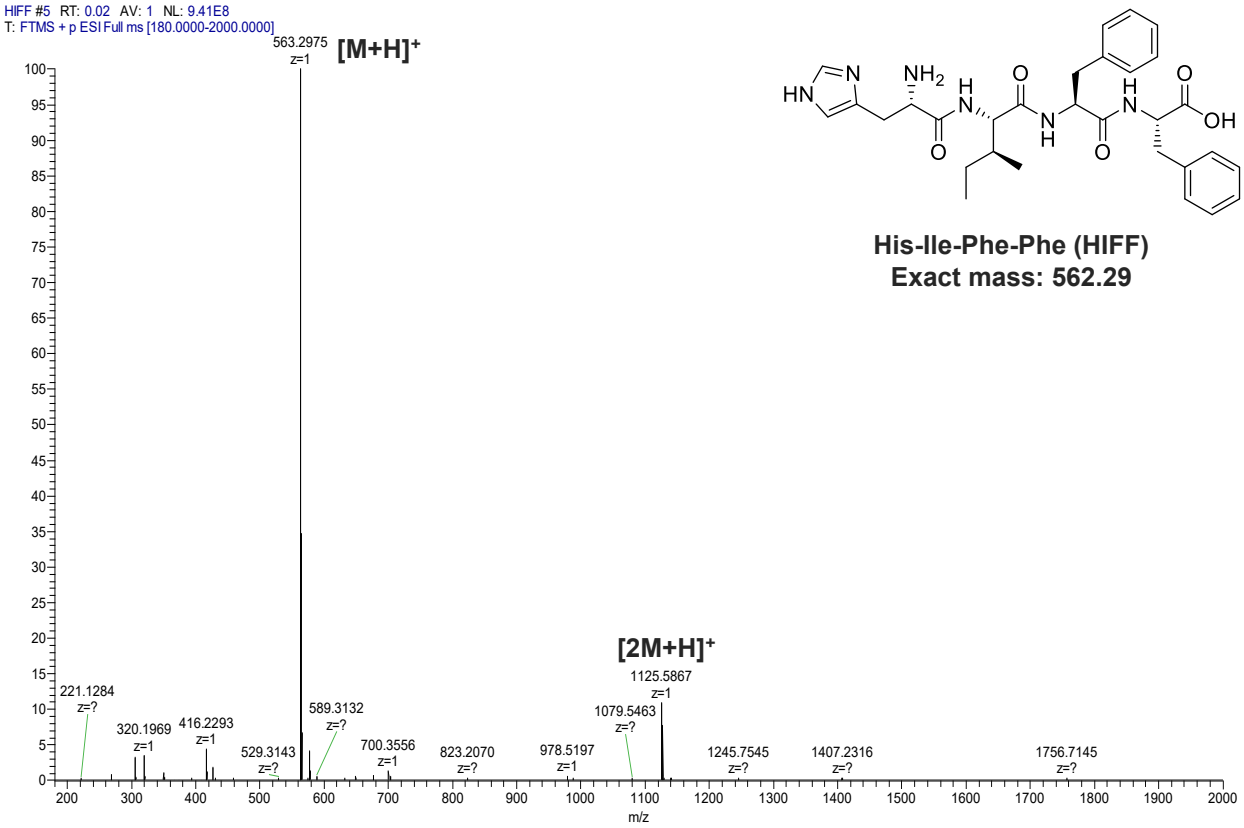

His-Ile-Phe-Phe (HIFF)
Exact mass: 562.29

Fig. S4 ESI-TOF MS spectrum of the synthesized peptide HIFF

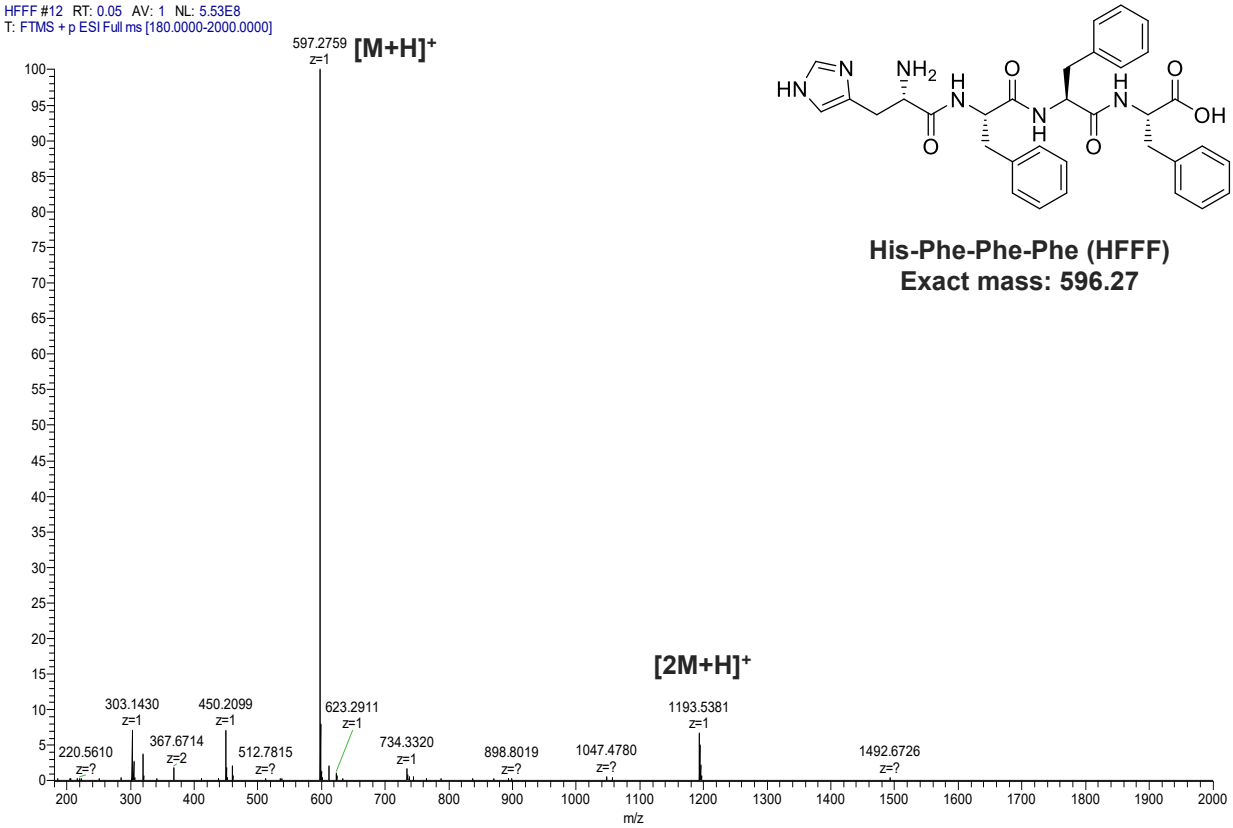

His-Phe-Phe-Phe (HFFF)
Exact mass: 596.27

Fig. S5 ESI-TOF MS spectrum of the synthesized peptide HFFF

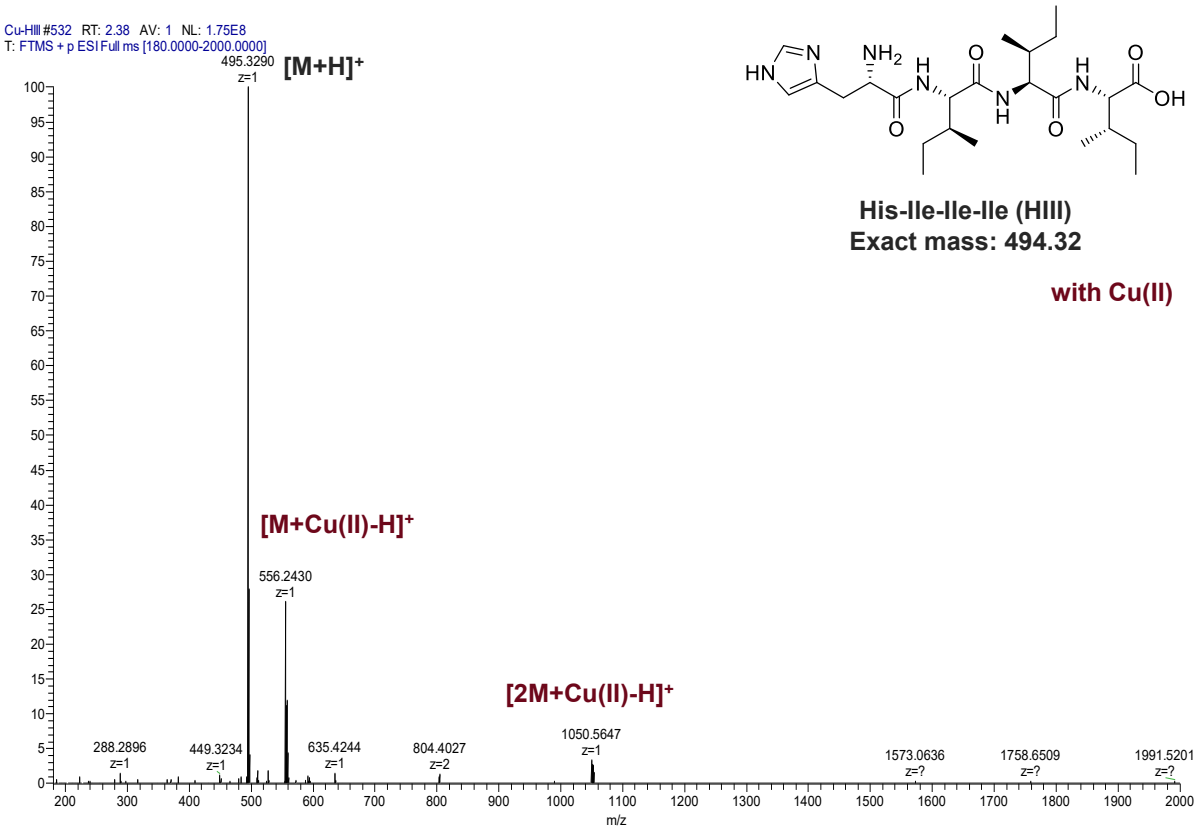

Fig. S6 ESI-TOF MS spectrum of the synthesized peptide Cu–HIII

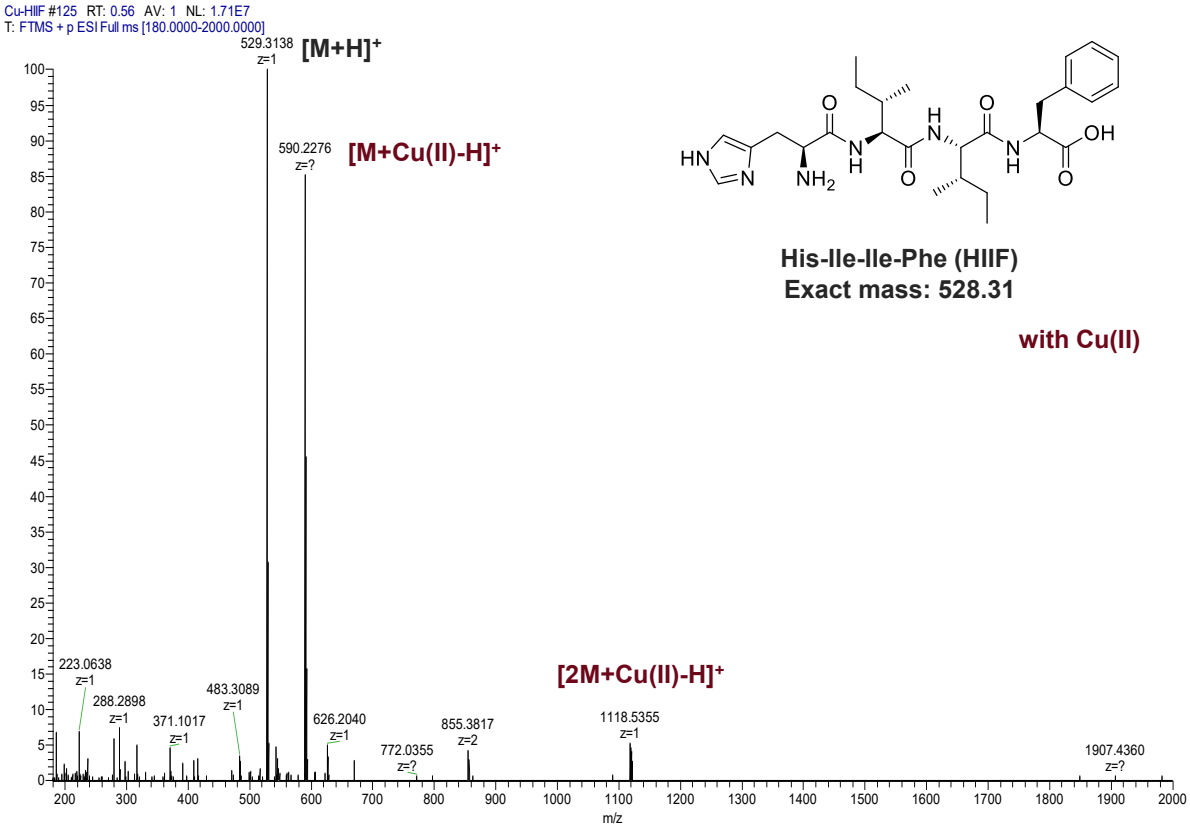

Fig. S7 ESI-TOF MS spectrum of the synthesized peptide Cu–HIIF

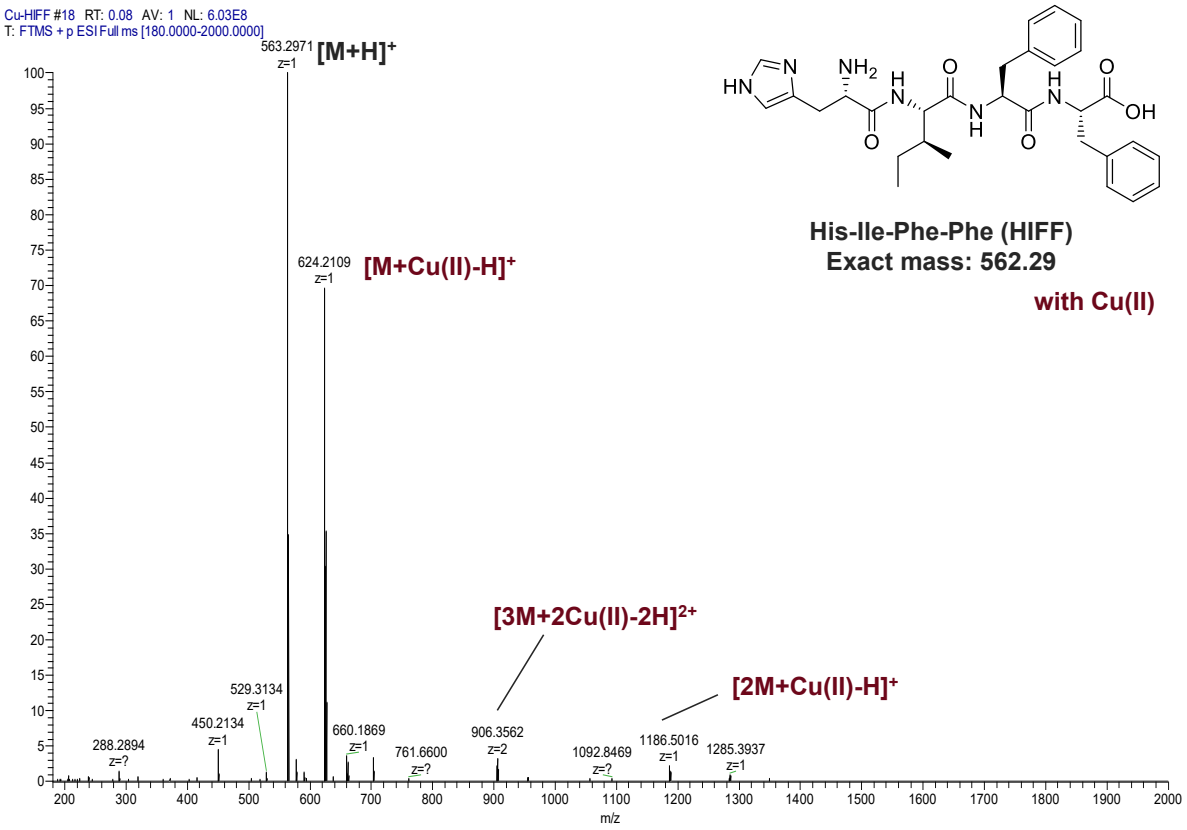

Fig. S8 ESI-TOF MS spectrum of the synthesized peptide Cu–HIFF

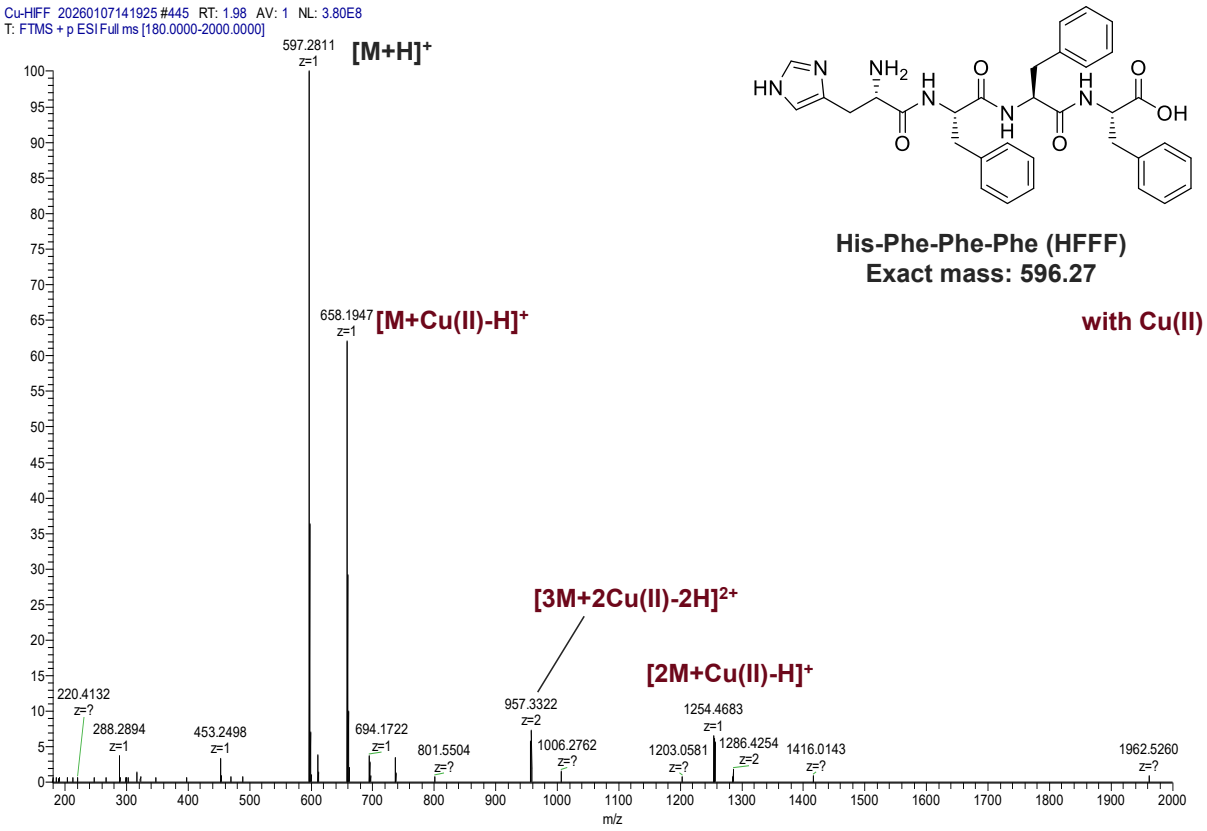

Fig. S9 ESI-TOF MS spectrum of the synthesized peptide Cu–HFFF

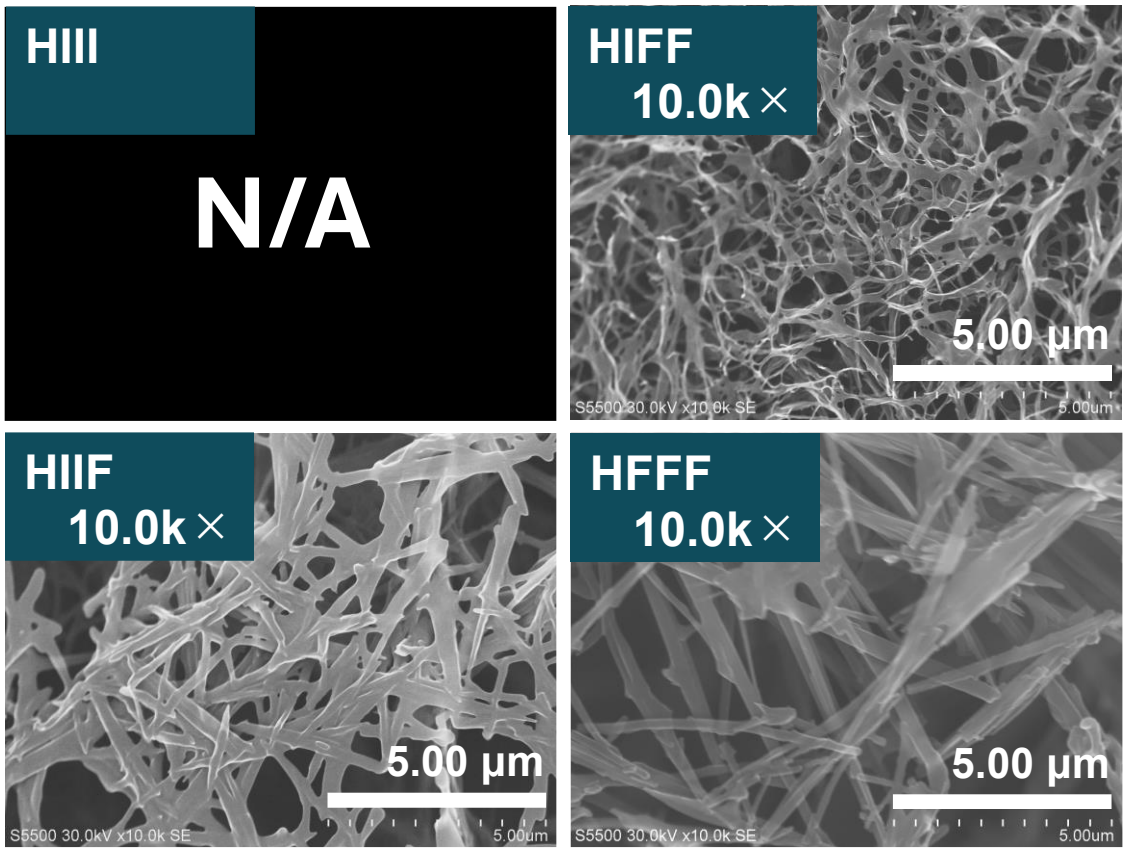

Fig. S10 Representative SEM images of the HIIF, HIFF, and HFFF nanostructures (10,000× magnification); HIII was completely soluble in water and did not form aggregates; therefore, SEM images were not obtained.

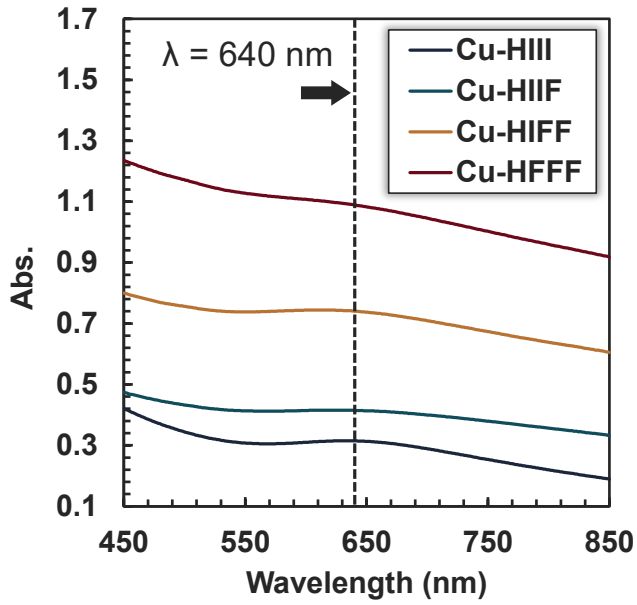

Fig. S11 UV-vis spectra of Cu–HIII, Cu–HIIF, Cu–HIFF, and Cu–HFFF solutions at 450–850 nm

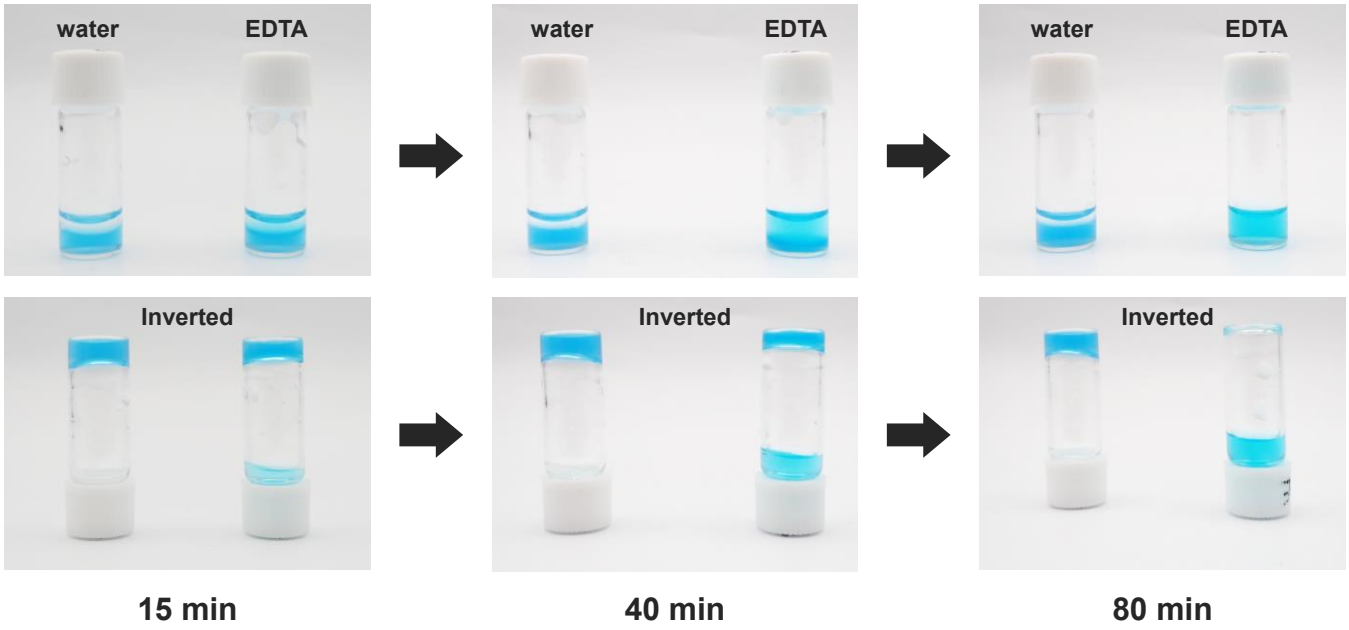

Fig. S12 Representative photographs of the Cu–HIIF metallogel after the addition of an equal volume of water or 50 mM EDTA aqueous solution; the EDTA-treated gel completely dissolved within 80 min, whereas no noticeable change was observed in the water-treated sample.

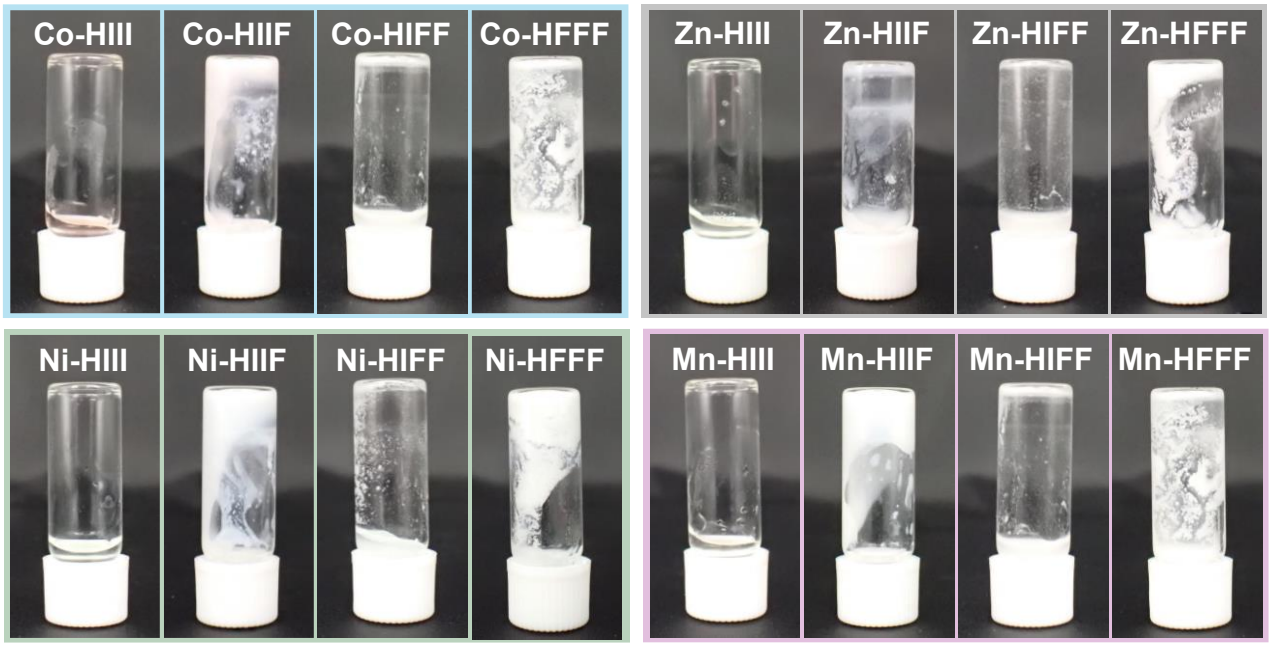

Fig. S13. Metal-ion selectivity of gel formation. Photographs of the four tetrapeptide samples after addition of Co^{2+}, Ni^{2+}, Zn^{2+}, and Mn^{2+} under the same preparation conditions. Gel formation was observed only in the presence of Cu^{2+}, whereas the tested metal ions other than Cu^{2+} did not induce gelation.

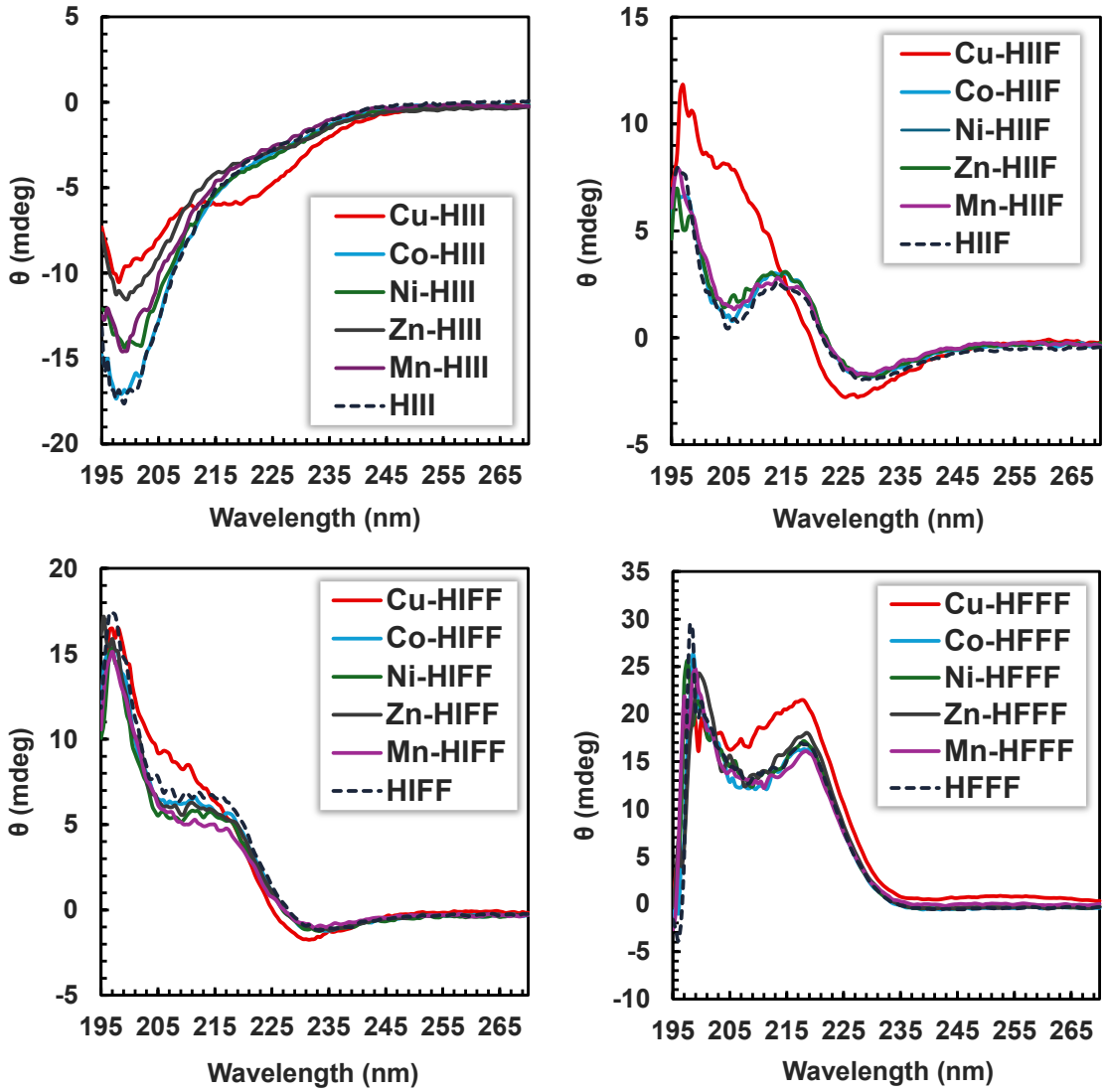

Fig. S14. CD spectral changes of the tetrapeptides in the presence of different metal ions. CD spectra of the four tetrapeptides after addition of Cu^{2+} and other metal ions under the same conditions. Compared with the pronounced spectral changes observed upon Cu^{2+} addition, the other metal ions induced only minor changes, indicating that Cu^{2+} is particularly effective in promoting the conformational transition associated with supramolecular gelation.